

EXPERIMENTAL STUDY OF TURBULENT STRUCTURE OVER PERMEABLE WALLS WITH A REFRACTIVE-INDEX-MATCHING TECHNIQUE

Taehoon Kim

Department of Mechanical Science
and Engineering
University of Illinois at Urbana-Champaign
MEB, 1206 W. Green St. Urbana, IL 61801, USA
tkim91@illinois.edu

James Best

Department of Geology

University of Illinois at Urbana-Champaign
605 E. Springfield Ave. Champaign, IL 61801, USA
jimbest@illinois.edu

Gianluca Blois

Department of Aerospace and Mechanical
Engineering
University of Notre Dame
118 Hessert Lab. Notre Dame, IN 46556, USA
gblois@nd.edu

Kenneth T. Christensen

Department of Aerospace and Mechanical
Engineering
University of Notre Dame
374 Fitzpatrick Hall, Notre Dame, IN 46556, USA
christensen.33@nd.edu

ABSTRACT

High-resolution particle velocimetry (PIV) measurements were conducted to explore turbulent flow overlying idealized permeable walls. The measurements successfully captured the overlying flow as well as the flow within the pore spaces with the specific goal of investigating the flow interactions across the permeable interface. A refractive-index matching (RIM) technique was employed to gain full optical access to the near-wall and subsurface flow and a number of idealized wall models were fabricated by casting acrylic. The permeable walls consisted of two and five layers of cubically packed uniform spheres ($d=25.4\text{mm}$), which provided 48% of porosity. In addition, an impermeable rough wall with identical topography was considered as a baseline of comparison in order to explore the structural modifications imposed by the permeability in the near-wall region. First- and second-order velocity statistics at two specific locations provided a quantitative assessment of such modifications of the local flow. A double-averaging approach (Nikora et al., 2007) allowed investigation of the global representation of the flow and to assess conventional scaling parameters.

INTRODUCTION

Turbulent flow overlying permeable walls is encountered in a wealth of environmentally- and industrially-relevant systems across seemingly disparate fields of science and engineering. Particularly in natural systems, permeable interfaces are ubiquitous across a broad range of scales (Ghisalberti, 2009), spanning from small-scale biological interfaces (Khakpour and Vafai, 2008) to large-scale geophysical systems such as alluvial river beds (Best, 2005, Blois et al., 2012) and aquatic and atmospheric canopies (Raupach et al., 1996, Nepf, 2012) in which turbulence is actively involved in morphodynamic as well as environmental processes. However, despite the critical technological and social implications of these flows and decades

of research focused on developing representative theoretical and numerical models, the physics of permeable-wall turbulence remains poorly understood.

A wall-bounded turbulent flow system that includes a permeable wall can be subdivided into two distinct flow regions, separated by a porous interface. The first is the surface (or free) flow, which overlies the interface. The second is the subsurface (or pore) flow, which occurs through the permeable wall. While the near-wall surface flow can be turbulent, deep within the subsurface, the flow tends to be laminar and can be described by Darcy's law (a balance of viscous and pressure forces). A region must exist between these two extremes where the flow undergoes a transition from turbulent to laminar across the permeable interface. This region, termed the "transitional layer," is marked by significant momentum and energy exchange and is the focus of increasing scientific interest. While the near-wall surface flow is similar to that of a boundary layer overlying an impermeable surface, wall permeability introduces new characteristic scales and complex flow mechanisms promoted by the slip and penetration conditions at the permeable interface.

Alluvial river beds, which are the inspiring systems of this work, can be modeled as permeable walls with a rough interface. Due to the presence of significant subsurface flow through the uncohesive grains (hyporheic zone), the near-bed flow is conceptually different from the canonical notion of flow over an impermeable rough wall. The near-bed hyporheic flow is driven by the interplay between the roughness (i.e. grains at the bed interface protruding into the free flow) and the permeability (interstitial fluid-filled spaces in the porous structure). The current effort explores the differences in turbulent flow overlying an idealized highly permeable rough wall which mimics a coarse-grained river bed and an impermeable wall of identical topography.

Wall permeability drastically enhances the friction factor at the permeable interface compared to flow over impermeable surfaces. Zagni and Smith (1976) performed pitot-tube

measurements in an open channel flow over a permeable wall constructed of spheres. They reported that the friction factor (f) over the permeable wall was higher than that produced by an impermeable wall of identical topography. A similar effect was also reported by Kong and Schetz (1982) and Zippe and Graf (1983). This increase in f is likely associated with the enhanced energy dissipation across the permeable interface owing to momentum exchange between the pore flow and the free flow. More recently, several investigations demonstrated that the increment of the friction factor is accompanied by modifications of the near-interface flow structure. The degree of wall porosity and the wall thickness are key parameters in controlling such modifications as they alter the intensity of the interactions (Breugem et al., 2006, Suga et al., 2010, Manes et al., 2011). Breugem et al. (2006) performed direct numerical simulations (DNS) of turbulent channel flow with varying permeability. In their approach, they were able to control the interface characteristics (i.e. topography). Using numerical artifacts, they maintained smooth-wall conditions in order to avoid unwanted roughness effects and noted the disappearance of quasi-streamwise near-wall streaks when the wall porosity was high ($\phi=95\%$). Despite the technical challenges in replicating this observation experimentally, Suga et al. (2010) and Manes et al. (2011) performed measurements of flow over a layer of foam. Their results corroborated the notion that wall permeability induces structural modifications of the turbulent boundary layer. Such modifications include the shape of the velocity profiles as well as the statistical distribution of turbulent events.

One of the most controversial aspects of the flow over permeable walls is the existence of Townsend's hypothesis of outer-layer similarity (Townsend, 1980) in the free flow. For example, Breugem et al. (2006) reported that such a condition was not achieved in their simulations, owing to the weakened wall blocking effect of the permeable wall with the highest porosity. On the other hand, more recent laser Doppler anemometry (LDA) measurements in an open channel flow with a foam type porous bed (Manes et al., 2011) showed self-similarity in the outer layer for both the mean and turbulence intensity profiles. Manes et al. (2011) attributed the occurrence of this outer-layer similarity to the relatively higher Reynolds

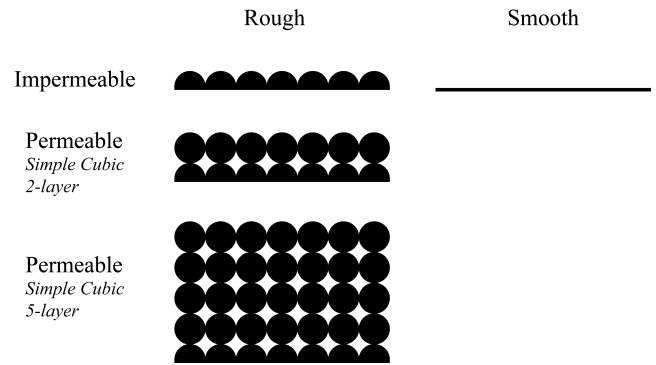


Figure 1. Schematic representation of wall models

number (Re) of their experiments coupled with the much higher ratio between shear penetration depth and the boundary layer thickness as compared to that of Breugem et al. (2006).

Exploring turbulent flow above and within a porous bed is challenging both numerically and experimentally. One of the major experimental challenges is that physical and optical access to the pore space is almost always limited. Optical diagnostic methods such as particle image velocimetry (PIV) could be used in combination with transparent porous walls; however, optical aberrations due to light refraction at the solid-fluid interface introduce unacceptable measurement bias. To overcome these challenges, a technique known as refractive index matching (RIM) was employed in the current investigation. Accurate index matching between the working fluid and the transparent permeable wall model allowed unaberrated optical access to both the near-wall flow and the flow *within* the porous subsurface.

The goal of the current study is to experimentally explore the role of permeability in the surface-subsurface turbulent interaction across the interface of a packed bed. For this purpose, two individual questions were set to systematically fulfill the investigation: 1) How does wall permeability impact the surface flow and modify the overlying boundary layer? And 2) How do the surface and subsurface flows interact across the wall interface? In answering these questions, it is necessary to examine the geometrical aspects of the packed bed that can play a role into

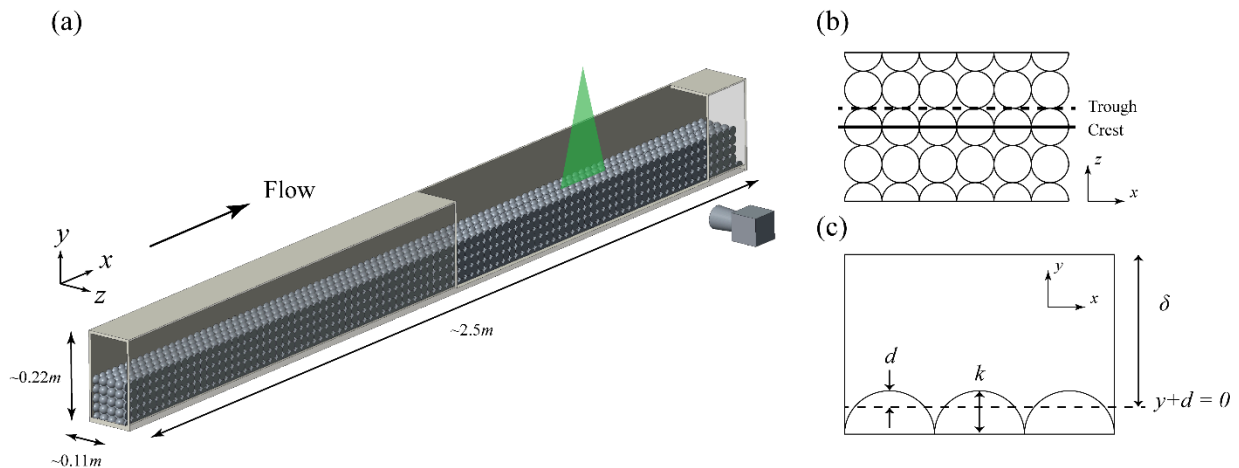


Figure 2. Schematic illustration of (a) PIV experimental setup, (b) two spanwise measurement locations, and (c) the length scales associated with the virtual origin offset (dashed-line)

Table 1. Experimental parameters based on double-averaged flow quantities

	k	k^+	d	$\langle \bar{U} \rangle_e$	δ	u_τ	Re_τ	Re_θ	Symbol
	(mm)		(mm)	(m/s)	(mm)	(m/s)			
Smooth				1.02	25.5	0.0360	880	2,730	✱
Impermeable Rough	12.7	382	2.7	0.59	46.6	0.0337	1,430	3,540	○
Permeable Rough (2-layer)	12.7	398	2.7	0.61	47.8	0.0345	1,500	3,600	◇
Permeable Rough (5-layer)	12.7	344	3.8	0.44	56.6	0.0298	1,530	3,340	□

the interface dynamics. Wall models considered herein are an impermeable smooth wall, an impermeable rough wall, and 2- and 5-layer permeable rough walls, with the surface topography of the later three being identical (see Fig. 1). These wall models allow the effect of wall permeability as well as the wall thickness to be highlighted in the current experiments.

METHOD

All experiments were performed in the RIM flow facility at the University of Notre Dame (Blois et al., 2012) as illustrated in **Error! Reference source not found.**(a). The test section is 2.5m long and has a cross-sectional area of 0.11m (width) by 0.22 m (height). For each experiment, a wall model with uniform characteristics was fixed at the bottom of the test section over its entire length. The cross section of the free flow was kept constant (0.11 by 0.11m) by arranging the top side of the wall (i.e. wall interface) at the same elevation for all cases.

All wall models were cast using an acrylic resin ($RI = 1.498$ at 25°C). The basic geometrical element of the idealized wall was a sphere (25.4 mm diameter). In constructing the wall models, three main geometrical parameters were considered: i.) *wall porosity*, ii.) *wall roughness* and iii.) *wall thickness*. The models are schematically presented in Figure 1. Spheres were packed in a cubic arrangement and the porosity of all permeable cases was 48%.

For the rough-wall cases, the roughness height, k , was uniform and equal to the radius of the spheres ($k = 12.7$ mm). The thickness of the boundary layer, δ , was approximately 50 mm. This provided, a relatively large roughness height to TBL thickness, $\delta/k \sim 4$. While this low-submergence flow condition ($k < \delta < (2-5)k$ by definition of Nikora et al. (2001)) produced a rather low spatial scale separation, it remains relevant to a broad range of environmental flow processes. The solid phase was rendered invisible by immersing it in an aqueous solution of sodium iodide (NaI, $RI \sim 1.495$ at 25°C) and by fine-tuning its RI through adjustment of fluid temperature.

High-resolution 2D PIV measurements in the streamwise-wall-normal (x - y) plane were performed at two spanwise locations (one is along the crest top of the roughness, and the other is along the trough between neighboring spheres) as depicted in **Error! Reference source not found.**(b). A double-averaging method (Nikora et al., 2007) was used to combine these two data sets and obtain a global representation of the flow to characterize the flow parameters. The experimental parameters

based on double-averaged flow quantities are summarized in Table 1.

RESULTS

The first objective was to estimate the location of the virtual origin (or *zero-plane displacement*, d) and the friction velocity (u_τ), which are utilized for data normalization and comparison. Due to the low-submergence flow condition investigated herein, the accuracy of the outer length scale $(y + d) / \delta$ is sensitive upon the estimation of the virtual origin. Herein, d was estimated by best-fitting the logarithmic region of the double-averaged velocity profile. For the impermeable rough-wall cases, d is located at an elevation of about $0.21k$ below the crest top. This value is consistent with previous studies employing the same cubic-packed array of hemispheres (Grass et al., 1991, Bomminayuni and Stoesser, 2011). The virtual origin of the 5-layer permeable rough wall case, instead, resides at approximately $0.3k$ below the crest top, which is lower than that of the impermeable rough wall case due to the relaxation of the no-penetration boundary condition.

The turbulent boundary layer thickness, δ was estimated as the distance between the virtual origin and the location where the double-averaged profile reaches 99% of the free stream (see **Error! Reference source not found.**(c)). The modified Clauser chart method was used to estimate u_τ (Perry and Li, 1990). A validation based on the total stress method was also performed, and the difference in the friction velocity between the two methods is within 5% for all cases. The roughness sublayer is determined following Cheng and Castro (2002), as the elevation where the standard deviation of the double averaged Reynolds shear stress profile falls below 5%. By this definition, the upper boundary of the roughness sublayer is 0.6δ , 0.6δ and 0.2δ for the impermeable, 2-layer and 5-layer permeable rough wall cases, respectively.

After estimating the virtual origin, the impact of permeability on the near-wall flow is explored by investigating the local flow over three wall models with the same topography but different permeability (i.g. impermeable, 2-layer, and 5-layer permeable). For the sake of clarity, the term ‘local’ flow is used herein to refer to a streamwise-averaged flow along a given spanwise position (crest or trough). The study of the local flow for the permeable wall carries with it a particular importance. While the boundary conditions at the crest region are the same as an impermeable surface (no slip and no penetration), the trough region has an open permeable interface between the surface and subsurface

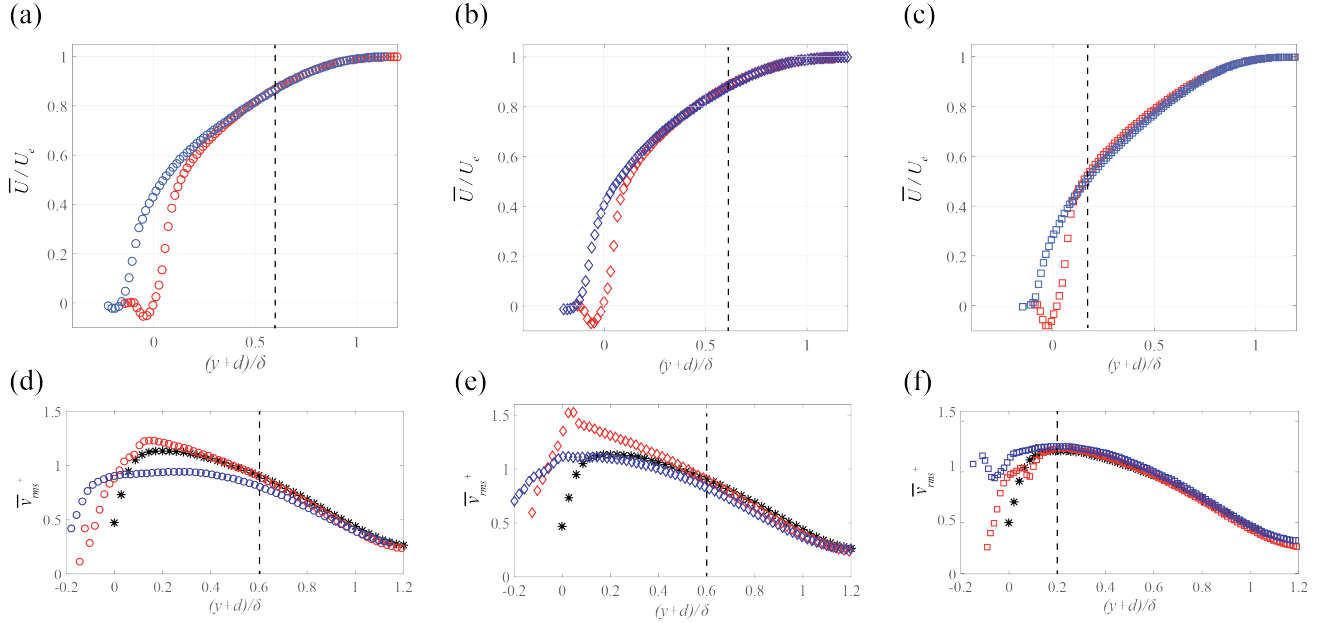


Figure 2. Local mean velocity profiles of (a) impermeable, (b) 2-layer permeable, and (c) 5-layer permeable rough wall. The rms of local wall-normal fluctuations of (d) impermeable, (e) 2-layer permeable, and (f) 5-layer permeable rough wall. The crest case is red, and the trough case is blue. The vertical dashed-line represents the upper boundary of the roughness sublayer.

flow region, allowing non-zero vertical flow. **Error! Reference source not found.**(a)-(c) show the local mean velocity profiles for three walls: impermeable, 2-, and 5-layer permeable rough. For all wall cases, the mismatch between the two local profiles is clearly visible, indicating the spanwise heterogeneity of the flow induced by the cubic-packed arrangement. The thickness of the roughness sublayer can be estimated as the location where the convergence of the local profiles occur. Our results suggest that the thicker the wall, the thinner the roughness sublayer. The mean flow on the crest region for all different walls is independent of the permeability and the wall thickness, indicating that the thinning of the roughness sublayer is controlled by the surface-subsurface momentum exchange processes that are concentrated at the trough.

The local near-wall turbulence is also considerably influenced by both permeability and wall thickness. The root-mean-square (rms) profiles of the local wall-normal velocity fluctuations in inner scaling are presented **Error! Reference source not found.**(d)-(f). The impermeable smooth wall case is included for comparison. The permeability effect is clearly noted on both the crest and trough regions of the 2- and 5-layer cases in the near-wall region. A significant increase in fluctuations is observed in the trough region owing to the open permeable interface along the trough side where momentum and scalar exchange occurs. The wall thickness also plays a crucial role to modify the near-wall turbulence structure. The crest region for the 5-layer case undergoes a reduction in stress close to the wall, while the 2-layer case behaves in the opposite way showing an increase in stress. This opposite behavior for the 2-layer permeable wall is due to the fact that the no-penetration boundary condition is not sufficiently relaxed as compared to that of 5-layer permeable wall. In this regard, the structural behavior of the local wall-normal fluctuations for the 2-layer permeable wall is more similar to the impermeable rough wall showing a strong spatial

heterogeneity in the near-wall region. The 5-layer case, on the other hand, has better flow homogenization close to the wall due to the deeper wall thickness, resulting in a thinning of the roughness sublayer. For the trough case of the 5-layer permeable wall, a strong secondary peak near the wall is observed. Thus, our results indicate that the permeable wall with a deeper wall thickness induces a more energetic vertical exchange of momentum, energy, and scalars through the permeable interface as compared to the one with a shallow wall thickness.

Despite a significant impact of the permeability and the wall thickness on the near-wall flow structure, local flow quantities (i.e. mean velocity and Reynolds stresses herein) for current wall models show a good collapse in the outer region on that of the impermeable smooth wall. For instance, the velocity defect form for each wall case (not shown herein for brevity) has an excellent agreement with the impermeable smooth wall profiles after the upper boundary of the roughness sublayer. Furthermore, the local wall-normal Reynolds stresses presented in Figure 2(d)-(f) display a similar behavior in structure to the impermeable smooth wall case in the outer region independent of permeability and wall thickness. This similarity is consistently found in other Reynolds stress components. These observations are in contradiction with the classical notion of outer-layer similarity. As reported by Jimenez (2004), a δ/k threshold for the scale separation resulting in the wall-similarity is 40 or more, which is much larger than the one in the current flow conditions ($\delta/k \sim 4$). However, recent studies revealed statistical evidence of wall-similarity both in the mean and turbulence structure with various large three-dimensional roughness with δ/k much lower than 40 (Connelly et al., 2006, Singh et al., 2007, Amir and Castro, 2011, Bomminayuni and Stoesser, 2011). Moreover, for the flow overlying a permeable wall, the presence of wall similarity is also reported by Manes et al. (2011). Therefore, we speculate that the

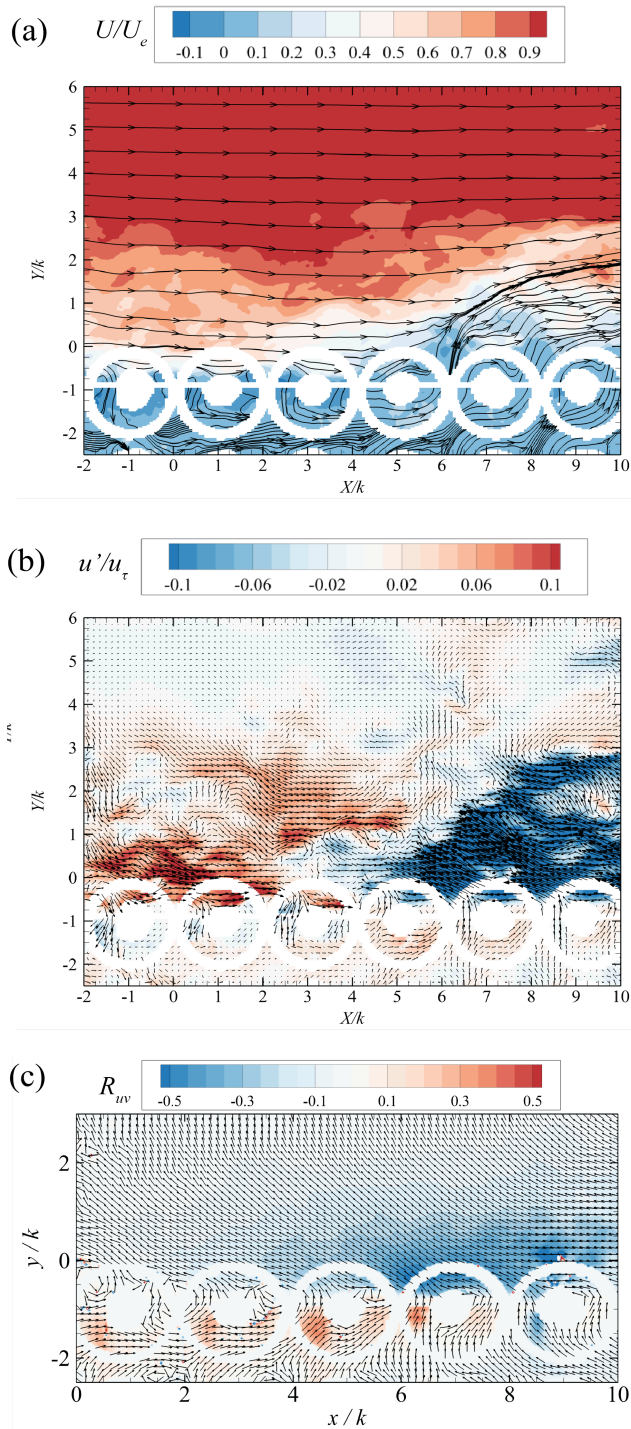


Figure 3. Contour map of (a) instantaneous streamwise velocity field superimposed with streamlines, (b) the corresponding instantaneous streamwise fluctuation field superimposed with fluctuation vectors, and (c) conditional average of u'_j given by $v' > 0$ at the permeable interface. The trough region of the 5-layer permeable rough wall is considered herein.

influence of permeability coupled with the surface roughness is confined within the roughness sublayer.

To explore the flow interaction between the surface and subsurface flows, the instantaneous streamwise velocity and fluctuation fields are examined for the 5-layer permeable rough wall at the trough region (see **Error! Reference source not found.**(a) and (b), respectively). Here, the y origin resides at the crest top and the y -coordinate is normalized by the roughness height, k . The streamlines in **Error! Reference source not found.**(a) show a clear upwelling flow from the pore space into the free flow region. This event is associated with low-momentum fluid ($u' < 0$) above the interface, while high-momentum fluid is prevalent below the interface. This observation indicates that the low-momentum fluid, seen to induce a large-scale ejection event, accelerates the pore-space flow. These jets of fluid into the surface flow region, cause a momentum deficit of the near-wall flow compared to the rough impermeable wall case. In contrast, when the down-welling flow occurs and turbulence penetrates into the pore space, high- and low-momentum fluid are dominant in the surface and subsurface flow region, respectively (not shown herein for brevity). Our findings suggest that near-interface surface and subsurface flow are thus negatively correlated.

To statistically investigate such flow interactions across the wall interface, conditional averaging was carried out using linear stochastic estimation (LSE). **Error! Reference source not found.**(c) displays a contour map of the conditional average of u'_j given a $v' > 0$ event near the permeable interface ($x/k = 6$ and $y/k = -0.75$). The contour map shows that the upwelling event across the wall interface is statistically consistent with low- and high-momentum fluid in the surface and subsurface flow regions, respectively. Similarly, the occurrence of down-welling flow across the permeable interface comes with the dominance of high- and low-momentum fluid in the surface and subsurface flow regions, respectively. These statistical observations support a previous study (Breugem et al., 2006) which reported a link between the penetrating flow across the permeable interface and the transporting fluid in the surface flow region with respect to the sign of the fluctuating velocity component. Based on the statistical evidence from the current conditional averaging, it can be thus inferred that the large-scale structures in the surface flow regions modulate the structures in the subsurface pore flow.

CONCLUSION

High-resolution 2D PIV measurements coupled with the RIM technique have been conducted for impermeable and permeable walls. Using idealized wall models, representing impermeable and permeable rough walls with identical topography, the impact of the permeability and wall thickness on the flow interaction across the permeable interface were investigated. As expected for the cubic-packed arrangement of spheres (hemispheres), spanwise heterogeneity was found in the near-wall flow field over both the impermeable and permeable walls. Surface roughness seems to have a prevailing influence. However, permeability plays a crucial role to homogenize the flow, diminishing the spatial heterogeneity and thus thinning the extent of the roughness sublayer.

Wall permeability increases the near-wall stress along the trough region by allowing mass and momentum exchange across the interface. Despite the spatial heterogeneity induced by the

surface roughness and wall permeability, the flow over the current wall models showed a reasonably good agreement with the smooth-wall flow in the outer layer. Finally, instantaneous events of upwelling and down-welling flow across the permeable interface were captured, offering insight into the dynamics of the flow interaction between the surface and subsurface flows. Our data suggest that near-interface surface and subsurface flow are negatively correlated. The conditional averaging further confirms that low-momentum surface flow is associated with high momentum pore flow and upwelling across the interface and vice versa. Thus, it is likely that the free-flow structure actively modulates the flow within the pore space in a consistent manner.

REFERENCES

- AMIR, M. & CASTRO, I. P. 2011. Turbulence in rough-wall boundary layers: universality issues. *Experiments in Fluids*, 51, 313-326.
- BEST, J. 2005. The fluid dynamics of river dunes: A review and some future research directions. *Journal of Geophysical Research: Earth Surface (2003–2012)*, 110.
- BLOIS, G., CHRISTENSEN, K., BEST, J., ELLIOTT, G., AUSTIN, J., DUTTON, C., BRAGG, M., GARCIA, M. & FOUKE, B. A versatile refractive-index-matched flow facility for studies of complex flow systems across scientific disciplines. 50th American Institute of Aeronautics and Astronautics (AIAA) Aerospace Sciences Meeting, Nashville, TN, AIAA, 2012. 2012-0736.
- BOMMINAYUNI, S. & STOESSERT, T. 2011. Turbulence statistics in an open-channel flow over a rough bed. *Journal of Hydraulic Engineering*.
- BREUGEM, W., BOERSMA, B. & UITTENBOGAARD, R. 2006. The influence of wall permeability on turbulent channel flow. *Journal of Fluid Mechanics*, 562, 35-72.
- CHENG, H. & CASTRO, I. P. 2002. Near wall flow over urban-like roughness. *Boundary-Layer Meteorology*, 104, 229-259.
- CONNELLY, J., SCHULTZ, M. & FLACK, K. 2006. Velocity-defect scaling for turbulent boundary layers with a range of relative roughness. *Experiments in fluids*, 40, 188-195.
- GHISALBERTI, M. 2009. Obstructed shear flows: similarities across systems and scales. *Journal of Fluid Mechanics*, 641, 51-61.
- GRASS, A., STUART, R. & MANSOUR-TEHRANI, M. 1991. Vortical structures and coherent motion in turbulent flow over smooth and rough boundaries. *Philosophical Transactions of the Royal Society of London A: Mathematical, Physical and Engineering Sciences*, 336, 35-65.
- JIMENEZ, J. 2004. Turbulent Flows over Rough Walls. *Annual Review of Fluid Mechanics*, 36, 173-196.
- KHAKPOUR, M. & VAFAI, K. 2008. Critical assessment of arterial transport models. *International Journal of Heat and Mass Transfer*, 51, 807-822.
- KONG, F. Y. & SCHETZ, J. A. 1982. Turbulent boundary layer over porous surfaces with different surface geometries. *AIAA paper*, 82-0030.
- MANES, C., POKRAJAC, D., NIKORA, V., RIDOLFI, L. & POGGI, D. 2011. Turbulent friction in flows over permeable walls. *Geophysical Research Letters*, 38.
- NEPF, H. M. 2012. Flow and transport in regions with aquatic vegetation. *Annual Review of Fluid Mechanics*, 44, 123-142.
- NIKORA, V., GORING, D., MCEWAN, I. & GRIFFITHS, G. 2001. Spatially averaged open-channel flow over rough bed. *Journal of Hydraulic Engineering*.
- NIKORA, V., MCEWAN, I., MCLEAN, S., COLEMAN, S., POKRAJAC, D. & WALTERS, R. 2007. Double-averaging concept for rough-bed open-channel and overland flows: Theoretical background. *Journal of Hydraulic Engineering*.
- PERRY, A. & LI, J. D. 1990. Experimental support for the attached-eddy hypothesis in zero-pressure-gradient turbulent boundary layers. *Journal of Fluid Mechanics*, 218, 405-438.
- RAUPACH, M. R., FINNIGAN, J. & BRUNEI, Y. 1996. Coherent eddies and turbulence in vegetation canopies: the mixing-layer analogy. *Boundary-Layer Meteorology*, 78, 351-382.
- SINGH, K., SANDHAM, N. & WILLIAMS, J. 2007. Numerical simulation of flow over a rough bed. *Journal of Hydraulic Engineering*, 133, 386-398.
- SUGA, K., MATSUMURA, Y., ASHITAKA, Y., TOMINAGA, S. & KANEDA, M. 2010. Effects of wall permeability on turbulence. *International Journal of Heat and Fluid Flow*, 31, 974-984.
- TOWNSEND, A. A. 1980. *The structure of turbulent shear flow*, Cambridge university press.
- ZAGNI, A. F. & SMITH, K. V. 1976. Channel flow over permeable beds of graded spheres. *Journal of the Hydraulics Division*, 102, 207-222.
- ZIPPE, H. J. & GRAF, W. H. 1983. Turbulent boundary-layer flow over permeable and non-permeable rough surfaces. *Journal of Hydraulic research*, 21, 51-65.